

## Application of Differential Anomalous X-Ray Scattering to Structural Studies of Amorphous Materials

P. H. Fuoss and P. Eisenberger  
Bell Laboratories, Murray Hill, New Jersey 07974

and

W. K. Warburton and A. Bienenstock  
Department of Materials Science, Stanford University, Stanford, California 94305  
(Received 22 January 1981)

A differential anomalous x-ray scattering technique has been developed for structural studies of disordered and amorphous systems. The results on amorphous GeSe<sub>2</sub> are consistent with the twofold coordination of Se and the fourfold coordination of Ge. The results on amorphous GeSe are consistent with threefold-coordinated models of the structure but not with the fourfold-twofold models.

PACS numbers: 61.40.Df, 61.10.-i

We report here the first implementation of a technique which uses anomalous x-ray scattering to determine the atomic coordinations of individual atomic species in polyatomic amorphous and disordered crystalline materials. This technique uses sharp changes in x-ray scattering amplitudes near characteristic absorption edges to isolate the scattering associated with a particular type of atom. This yields information qualitatively similar to extended x-ray-absorption fine-structure (EXAFS) analysis but includes low- $k$  information and, thus, long-distance correlations. The basic conceptual approach is due to Shevchik,<sup>1</sup> but a significantly different experimental approach was required to actually achieve meaningful results because of x-ray Raman scattering. We have used this method to determine the short-range coordinations of Ge and Se in amorphous GeSe, a topic of considerable debate for over ten years.

In normal radial-distribution-function (RDF) analysis, Fourier transformation of  $I(k)$ , the normalized scattered intensity, yields a weighted sum of all the pair distribution functions ( $\rho_{\alpha\beta}$ ). For polyatomic materials, it is often impossible to convert this sum into a unique structural model because one cannot uniquely determine the atomic pairs which contribute to a specific peak in the RDF. This is the case for amorphous GeSe in which Ge-Ge, Ge-Se, and Se-Se near-neighbor distances are expected to be almost identical. Similar problems occur for amorphous GeS, GeTe, and a number of other systems. For the germanium monochalcogenides, two quite different structural models are consistent with the RDF's as well as with other measurements. In the 2-4 model, proposed by Betts *et al.*,<sup>2</sup> each Ge

is fourfold and each Se twofold coordinated so that there must be Ge-Ge near-neighbor bonds at the stoichiometric composition. In the 3-3 model, discussed by Bienenstock,<sup>3</sup> each Ge (Se) is bonded to three Se (Ge) atoms so that there are no like-atom near neighbors in the defect-free structure. The differential-anomalous-scattering (DAS) technique used here allows us to resolve this ambiguity.

For amorphous and isotropic polycrystalline materials, the normalized x-ray scattering intensity can be written as<sup>4</sup>

$$I(k) = \sum_{\alpha} \sum_{\beta} \chi_{\alpha} f_{\alpha}(k) f_{\beta}^{*}(k) S_{\alpha\beta}(k). \quad (1)$$

Here  $\chi_{\alpha}$  and  $f_{\alpha}$  are, respectively, the atomic fraction and the complex atomic scattering factor of species  $\alpha$ ,  $k$  is the magnitude ( $4\pi \sin\theta/\lambda$ ) of the scattering vector,  $2\theta$  is the scattering angle,  $\lambda$  is the wavelength, and the  $S_{\alpha\beta}(k)$ , the partial structure factors, are given by

$$S_{\alpha\beta}(k) = (4\pi/k) \int_0^{\infty} [\rho_{\alpha\beta}(r) - \rho_{\beta 0}] r \sin(kr) dr. \quad (2)$$

The desired structural information is obtained from the pair distribution functions which are given by the expression

$$\rho_{\alpha\beta}(r) = N^{-1} \sum_{i=1}^{N_{\alpha}} \sum_{j=1}^{N_{\beta}} \delta(r_{ij} - r) / 4\pi r^2. \quad (3)$$

Here  $r$  is the interatomic separation,  $r_{ij}$  is the distance between atoms  $i$  and  $j$ , and  $N_{\alpha}$  is the number of atoms of species  $\alpha$  in the sample.  $\rho_{\beta 0}$  is the average density of  $\beta$  atoms.

The atomic scattering factor can be written as

$$f(k, E) = f_0(k) + f'(k, E) + if''(k, E), \quad (4)$$

where  $E$  is the photon energy,  $h\nu$ , and  $f_0(k)$  is

given by the Fourier transform of the atomic electron density.  $f''$ , being directly related to the absorption coefficient, is small and slowly varying for  $E$  below the edge, rises sharply at the edge, and then falls slowly.  $f'$  has a sharp negative peak at the edge with a width which is typically 40 to 60 eV at half minimum and is small elsewhere.

$$(\delta I(k)/\delta E)_k = \chi_A \sum_{\beta} (\delta/\delta E) [f_A(k) f_{\beta}^*(k) + f_A^*(k) f_{\beta}(k)] S_{A\beta}(k). \quad (5)$$

Fourier transformation of this derivative yields a weighted sum of the  $\rho_{A\beta}(r)$  and, therefore, information about the environment of the specific atomic species,  $A$ .

We measured the scattered intensity from a sputtered amorphous GeSe sample, 49% Ge–51% Se, as a function of photon energy and  $k$  near the Ge  $K$  absorption edge ( $E = 11\,000, 11\,040, 11\,080, 11\,090, 11\,095$ , and  $11\,100$  eV) and the Se  $K$  absorption edge ( $E = 12\,555, 12\,645, 12\,650$ , and  $12\,655$  eV). Similar data were acquired for a bulk quenched GeSe<sub>2</sub> glass at the same incident photon energies. The GeSe<sub>2</sub> data were used as a standard and a check on the data analysis procedure since its structure is relatively well understood.

All data were taken on beam line IV, at the Stanford Synchrotron Radiation Laboratory, which was equipped with a six-pole wiggler and a Si(220) two-crystal, parallel setting monochromator with an  $\sim 3.5$  eV bandwidth. The measurements at the Ge edge were performed with an angular receiving aperture of  $2 \text{ mrad} \times 40 \text{ mrad}$  and a NaI scintillation detector. At the Se edge, a flat graphite monochromator was used to eliminate the Ge fluorescence, part of the Se  $K$  fluorescence, and most of the Compton scattering.

The data analysis involved a five-step process which is described in more detail by Fuoss.<sup>5</sup> The steps were (1) removal of parasitic scattering, (2) correction for the system's angular response (e.g., due to sample length), (3) normalization of the data to an absolute per-atom basis, (4) subtraction of the normalized data sets to yield the DAS, and (5) Fourier transformation of the DAS [after multiplication by a convergence term  $\exp(-\sigma k^2)$ ] to obtain a differential distribution function (DDF). A significant improvement over the technique previously described by Fuoss was the weighting, in step 4, of the DAS by

$$\{\chi_A \Delta f' [\sum_{\beta} \Gamma_{\beta} \text{Re}(f_{\beta}(k, E_1) + f_{\beta}(k, E_2))] / 2\}^{-1},$$

where  $\Delta f'$  is the change in  $f'$  between the two en-

The DAS method used here takes advantage of the fact that  $f'$  and  $f''$  change rapidly only within  $\sim 100$  eV of an absorption edge and that the characteristic absorption edges are separated by several hundred to thousands of eV in the x-ray region. As a result, a derivative of Eq. (1) with respect to photon energy near the  $A$  atom's absorption edge yields, with use of  $\chi_A S_{A\beta} = \chi_{\beta} S_{\beta A}$ ,

ergies  $E_1$  and  $E_2$  and  $\Gamma_{\beta}$  is the estimated fraction of  $\beta$  in the first-neighbor peak. This weighting factor makes the peak areas in the DDF approximately equal to the coordination number.

The results are shown in Figs. 1 and 2. Fig. 1(a) shows the normalized differences (the result of step 4) between curves taken at 11 000 and 11 090 eV as a solid curve (the Ge  $K$  absorption edge is at 11 103 eV) ( $f_{\text{Ge}}' = -4.8$  and  $-9.0$ , respectively). The dashed curve is a similar dif-

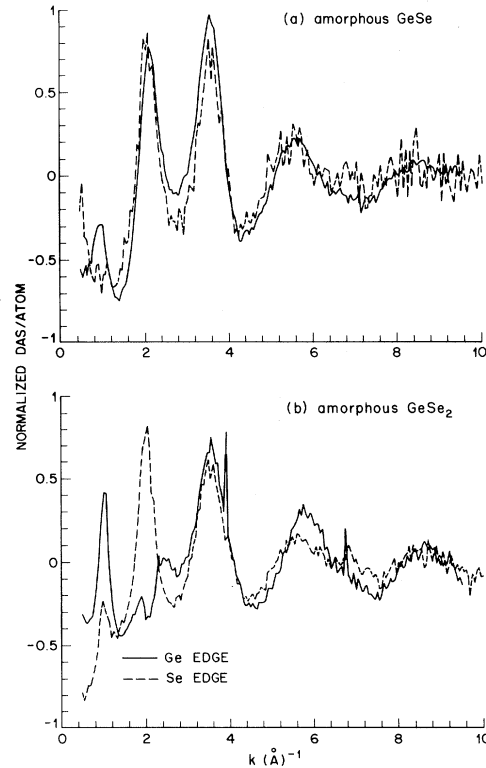


FIG. 1. The differential anomalous scattering (DAS) for (a) amorphous GeSe and (b) amorphous GeSe<sub>2</sub>. The solid curves are calculated with use of data taken at 11 000 and 11 090 eV and the dashed curves with use of data taken at 12 555 and 12 645 eV.

ference between curves for data taken at 12 555 and 12 645 eV (the Se  $K$  edge is at 12 656 eV ( $f_{\text{Se}}' = -4.9$  and  $-10.2$ , respectively)). While the Se edge DAS are noisier than the Ge edge DAS (because of the detector monochromator) these curves are quite similar to each other and to the total scattering from amorphous GeSe. As a result, we were concerned that the difference was merely reflecting a slight normalization error. The amorphous GeSe<sub>2</sub> data [similarly shown in Fig. 1(b)] lead us to reject that conclusion since the peak at  $\sim 2 \text{ \AA}^{-1}$  disappears at the Se edge and not the Ge edge.

These results were then Fourier transformed, leading to the DDF's shown in Fig. 2. All the DDF's show very small oscillations at low  $r$  similar to "good" RDF's. The GeSe first-neighbor peak areas were calculated to be 3.1 atoms for Ge and 2.5 atoms for Se. The Ge and Se first-neighbor distances (2.44 and 2.45  $\text{\AA}$ , respectively) agree very well. In addition, the second-neigh-

bor peaks are almost identical.

The results for GeSe<sub>2</sub> are shown in Fig. 2(b). The first-neighbor coordination numbers are 3.8 atoms for Ge and 2.3 atoms for Se. Again, the first-neighbor distances for Ge and Se (2.37  $\text{\AA}$  in both cases) are in excellent agreement. In contrast, the Ge DDF second-neighbor distance is  $\sim 0.09 \text{ \AA}$  shorter than the Se DDF distance. This is consistent with the  $sp^3$  coordination of Ge by Se yielding an ideal bond angle of  $109.5^\circ$  and the  $p^2$  coordination of Se by Ge with an "ideal" covalent-bond angle of only  $90^\circ$ . This phenomenon has been described for crystalline GeS<sub>2</sub> by Zachariasen,<sup>6</sup> and appears consistent with the model for the amorphous material of Aspnes *et al.*<sup>7</sup>

To estimate bounds on these results, we systematically varied  $f'$  and  $f''$  by  $\pm 20\%$ , the fit range in the normalization procedure, the types of first neighbors (in step 4), and the value of  $\sigma$  from 0.0 to  $0.03 \text{ \AA}^2$ . For Ge atoms, these changes modified the coordination number by  $\pm 0.2$  atoms in GeSe and  $\pm 0.4$  atoms in GeSe<sub>2</sub>. For Se atoms, the coordination number was changed by  $\pm 0.2$  atoms for GeSe and  $-0.4$  to  $+0.2$  atoms for GeSe<sub>2</sub>. In all cases, the first-neighbor coordination distance changed by  $< 0.02 \text{ \AA}$ .

While we have only shown one set of data here, the other data mentioned were analyzed and gave results which fall within the bounds discussed. In addition, data sets were taken near the Ge edge on amorphous GeSe on several different occasions (and presumably with different levels and types of systematic errors, e.g., those described by Fuoss<sup>5</sup>) and those data yield results that agree very well with these results.

The results imply strongly that the 3-3 model in which each Ge and Se is threefold coordinated is valid for amorphous GeSe. The derived coordination numbers are much more consistent with this model than with the 2-4 model in which Ge is fourfold and Se twofold coordinated. In addition, the Ge and Se DAS's and DDF's are quite similar in form for GeSe. This is to be expected from the very regular structure anticipated<sup>3</sup> for the 3-3 model but is not expected for the 2-4 model which necessarily contains either considerable chemical disorder or phase separation. Similarly, the 2-4 model would lead to different Ge and Se DDF second-neighbor peaks because of the differing bond angles, as seen for the GeSe<sub>2</sub> DDF's.

Since the results are very similar to those obtained, in principle, from an EXAFS analysis the major differences between the two techniques

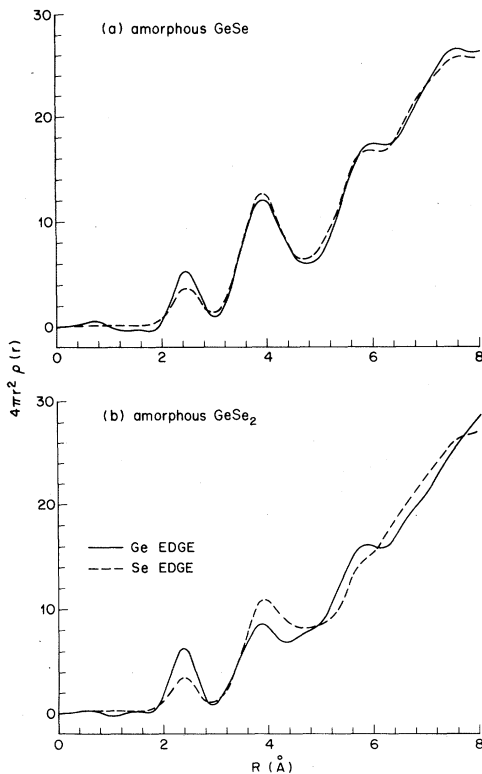


FIG. 2. The differential distribution functions (DDF's) for (a) amorphous GeSe and (b) amorphous GeSe<sub>2</sub>. The solid curves give the coordination of Ge atoms while the dashed curves give the coordination of Se atoms.

should be pointed out. First, a broad second-neighbor peak is clearly resolved in the DDF's and higher broad coordination shells are quite evident. Information on such broad shells cannot be obtained from EXAFS analysis because of the lack of low- $k$  information. Another advantage of DAS is that electron phase shifts and mean-free-path terms are not required. On the other hand, DAS is not as sensitive to the coordination of dilute species since it is obtained by looking at the difference between two large signals. Also, the DAS cannot be Fourier transformed to yield DDF's unless a fairly high energy-absorption edge is used (due to the limited  $k$  range available).

The current accuracy of DAS is mainly limited by inadequate knowledge of  $f'$ . The composition range is limited to, perhaps,  $> 5\%$ , except for heavy elements in a light matrix, and the elemental range to above Cr if  $k$  information beyond  $6 \text{ \AA}^{-1}$  is desired. This elemental limit applies mainly to Fourier transformation. Small- and low-angle scattering information useful for model building can be obtained on much lower- $Z$  materials. Thus we are confident that DAS can be successfully applied to a wide range of problems in structural analysis of amorphous materials, poorly crystallized materials, and materials on

low- $Z$  substrates (e.g., catalysts).

We would like to thank R. Flasck and Energy Conversion Devices for providing the sputtered GeSe sample and G. Brown and the Stanford Synchrotron Radiation Laboratory technical staff for their valuable assistance. This work was supported in part by the National Science Foundation through the Metastable Materials Thrust Program of the Center for Materials Research, Stanford University, and the experiment was performed at the Stanford Synchrotron Radiation Laboratory under Contract No. DMR-77-27489 (in cooperation with U. S. Department of Energy).

<sup>1</sup>N. J. Shevchik, *Philos. Mag.* **35**, 805, 1289 (1977).

<sup>2</sup>F. Betts, A. Bienenstock, D. T. Keating, and J. P. deNeufville, *J. Non-Cryst. Solids* **7**, 417 (1972).

<sup>3</sup>A. Bienenstock, *J. Non-Cryst. Solids* **11**, 447 (1973).

<sup>4</sup>B. E. Warren, *X-Ray Diffraction* (Addison-Wesley, Reading, Mass., 1969), Chap. 10.

<sup>5</sup>P. H. Fuoss, Ph.D. thesis, 1980, Stanford University, 1980 (unpublished), Stanford Synchrotron Radiation Laboratory Report No. 80/06, 1980.

<sup>6</sup>W. H. Zachariasen, *Phys. Rev.* **49**, 884 (1936).

<sup>7</sup>D. E. Aspnes, J. C. Phillips, K. L. Tai, and P. M. Bridenbraugh, *Phys. Rev. B* **23**, 816 (1981).

## Absolute Measurement of the (220) Lattice Plane Spacing in a Silicon Crystal

Peter Becker, Klaus Dorenwendt, Gerhard Ebeling, Rolf Lauer, Wolfgang Lucas, Reinhard Probst, Hans-Joachim Rademacher, Gerhard Reim, Peter Seyfried, and Helmut Siegert  
*Physikalisch-Technische Bundesanstalt, D-3300 Braunschweig, Federal Republic of Germany*  
(Received 3 February 1981)

The (220) lattice plane spacing of an almost perfect crystal of silicon was measured by means of a combined scanning (*LLL*) x-ray interferometer and a two-beam optical interferometer. From 170 measurements, a value  $d_{220} = (192\,015.560 \pm 0.012)$  fm results in vacuum at 22.50 °C. This value is smaller by  $1.8 \times 10^{-6} d_{220}$  than that reported by Deslattes *et al.* for another crystal. Generic variabilities of the two crystals account only for a part of this difference.

PACS numbers: 61.55.Dc, 06.30.Bp, 61.10.Fr

Bonse and Hart<sup>1</sup> proposed to measure the lattice plane spacing of crystals by means of a scanning x-ray interferometer and Bonse and te Kaat<sup>2</sup> observed x-ray fringes in a two-crystal (*LLL*) interferometer. Deslattes and Henins,<sup>3</sup> using this method, succeeded first in measuring the (220) lattice plane spacing of silicon with a stated uncertainty of  $3 \times 10^{-7}$ . The reported value has become the basis of the latest evaluation of charac-

teristic x-ray wavelengths ( $\text{Cu } K\alpha_1$  and  $\text{Mo } K\alpha_1$ ). An extended series of measurements with a reduced uncertainty led to a new value for the Avogadro constant.<sup>4</sup> The  $d_{220}$  value was corrected for systematic errors,<sup>5</sup> and its uncertainty finally reduced to  $1 \times 10^{-7}$ .<sup>6-8</sup>

In this paper, a new and significantly different value for  $d_{220}$  of silicon is reported. It was measured by the same method as before, but with a